6. CONCLUTION

This research was carried out based on a model of the power system of Sri Lanka, which was simulated suing PSCAD EMTDC and COMFORTRAN software. This power system simulation was done with reference to the load flow occurred on the 13th May, 2013 as the day-time peak demand, (around 12.30 p.m.). Different actual power system scenarios were simulated in this model and its results/performance was very much closer to real time values. But as I see, following are some points that should be accounted for, through which the performance of the simulation model could have been improved further.

- The power system is comprised with a variety of generator/ turbine types, such as steam – turbine power plants, gas – turbine power plants and diesel engines. In simulating these thermal generators in the power system, I have considered all of them (thermal generators) as steam turbine power plants. (Section 3.2.6.1)
- Even though the generation capacities are different I have used the same set of parameters in certain situations (especially in simulating the governor, turbine and generator) for thermal plants and hydro plants, (two separate sets for the two corresponding types). (Section 3.2.6.3, Section 3.2.7.2 Table 3.13, Table 3.16)
- It was not possible to get the actual inertia values for all generators, for the simulation. I used some experimental values as well as some calculated values in this process, which may not be the exact vales of the inertias of the units connected to the national grid at that instant. (Section 3.2.4.4, Table 3.10)
- In the simulation, the loads connected to bus bars at each grid were considered as fixed values. Even though the inductive and capacitive reactance varies with the system frequency variations, the option of inductive and capacitive loads which are not sensitive to system frequency was selected in the simulation.
- If we consider the construction details of a particular standard type underground cable, their construction details may be slightly different from one manufacturer to another. So the same values may not be applied in the simulation process, which are identical to the power system components.
- Devices such as CFL lamps, Variable Speed Drives, Switching devices etc. are becoming much popular in the country. Even though they have many advantageous situations to the consumer, on the other hand they introduce lot of harmonics whose

effects may be very bad for the utility as well as the power system. This issue has not been addressed in the simulation process.

With the developed simulation model of the Power System of Sri Lanka, it was able to come to certain conclusions which are much favorable to maintain the system with a high quality and reliable service. The results show that the Proposed Load Shedding Schemes are better solutions for the power system stability problem during generation deficiencies. These proposed load shedding schemes are exclusively specific for the power system of Sri Lanka. It depends on the electrical power system practice, regulations, largest generator capacity/capacities, electricity consumption pattern, capacity of embedded generation etc.

- By implementing a load shedding scheme at an initial stage of a generation deficiency, further reduction of system frequency can be eliminated. This would be very supportive in regulating frequency in a power system. Accordingly the proposing frequency for initiating a Load Shedding Scheme is 49. 4 Hz. With reference to the current practice of Sri Lanka, CEB initiates its Load Shedding Scheme if the system frequency < 48.75 Hz with a delay time of 100 ms.

- The chance of occurring the conditions "f < 49.0 Hz" and "-0.85 < df/dt" (which can be considered as adaptive to the system behavior) together (*i.e.* the logic condition 'f < 49.0 Hz & -0.85 < df/dt'), that are given in the CEB load shedding scheme is very much less. Hence there is a high possibility of initiating 'other stages' of the load shedding scheme in addition to this stage, which may lead to 'over-shedding'.

- If it is possible to limit implementing the load shedding stages in the Load Shedding Scheme only up to a system frequency of 48.6 Hz, the power system can be retained within the specified frequency limits (minimum safe operating frequency limit of thermal generator): *i. e.* the system frequency ≥ 47.0 Hz. Since Sri Lanka is a country which receives electricity mostly from thermal power generation, it is very important to keep the system frequency beyond the safe limit 47.0 Hz. Else this can lead for a catastrophic failure.

- Further by implementing disintegration of the national grid at an instant where the system frequency = 48.6 Hz, rather than considering a specific df/dt value, it is possible to maintain the frequencies in the national grid as well as in islands approximately above 47.5 Hz. There by the stability of the grid network can be assured.

- During disintegration of the power system it is very important to identify and isolate transmission lines which do not cater power to any loads but still energized while being connected to the power system. It is because this type of transmission lines can affect the reactive power balance of the power system and hence may lead to catastrophic failures.

  With the help of the simulation program I was able to explain real time situations/ problems which were experienced by engineers in the CEB,
  - while they were trying to isolate the southern part of the national grid
  - during a generation tripping occurred in the Laxapana and New-Laxapana power stations.

  This was because reactive power imbalances occur in the National Grid due to No-Load or Lightly Loaded transmission lines in the transmission network.

- With the Proposed LSS – II, even though it suggests 40% of the load to give priority in catering electricity (when concern the national grid) further amount of load receives power due to islanding operation. Therefore, it is possible to cater a larger number of consumers by disintegration of the power system.

- In this simulation model SVC were not used; instead by doing a small calculation for reactive power consumption in each island, the reactive power compensation was done. More successful results can be assured if SVCs were introduced to each and every island as well as to the national grid.

REFERENCES

[1] R. C. Dugan, M. F. McGranaghan, S. Santoso and H. W. Beaty, Electrical Power Systems Quality, Second Edition, McGraw-Hill, 2004.

[2] PUCSL, "Investigation Report on Power System Failures on 9th October 2009," Public Utilities Commision of Sri Lanka, 2010 February.

[3] J. Barkans and D. Zalostiba, Protection Against Black-outs and Self-restoration of Power Systems, Riga: RTU Publishing House, 2009.

[4] P. M. Anderson, Power system protection, IEEE press, Wiley-Interscience, 1999.

[5] Seimens, "Technical assesment of Sri Lanka's renewable resource based electricity generation, Final Report, RERED Project, Project No. 108763-0001," Seimens Power Technologies International Ltd, England, UK., 2005.

[6] J. Machowski, J. W. Bialek and J. R. Bumby, Power System Dynamics, Stability and Control, John Wiley & Sons, Ltd., 2008.

[7] P. Kundur, J. Paserba, V. Ajjarapu and G. Andersson, "Definition and Classification of Power System Stability, IEEE/CIGRE Joint Task Force on Stability Terms and Definitions," *IEEE TRANSACTIONS ON POWER SYSTEMS,* vol. 19, no. No. 2, pp. 1387-1401, MAY 2004.

[8] M. Q. Ahsan, A. H. Chowdhury, S. S. Ahmed, I. H. Bhuyan, M. A. Haque and H. Rahman, "Technique to Develop Auto Load Shedding and Islanding Scheme to Prevent Power System Blackout," *IEEE transactions on Power Systems,* vol. 27, no. No. 1, pp. 198-205, 2012.

[9] E. Vaahedi, Practical power system operation, IEEE press, Wiley, 2014.

[10] M. Giroletti, M. Farina and R. Scattolini, "A hybrid frequency/power based method for industrial load shedding," *Elsevier International Journal of Electrical Power and Energy Systems,* no. 35, pp. 194-200, 2012.

[11] P. Kundur, Power system stability and control, New York: McGraw-Hill, Inc., 1993.

[12] H. You, V. Vittal, J. Jung, C. Liu, M. Amin and R. Adapa, "An Intelligent Adaptive Load Shedding Scheme," in *14th PSCC*, Sevilla, Spain, 24-28 June, 2002.

[13] A. J. Wood, B. F. Wollenberg and G. B. Sheble, Power Generation, Operation, and Control, Third Edition, Hoboken, New Jersey: IEEE Press, Wiley, 2014.

[14] F. Saccomanno, Electric power systems, analysis and control, IEEE press, Wiley - Interscience, 2003.

[15] M. Eremia and M. Shahidehpour, Hand book of electrical power systemdynamics: modeling, stability and control, IEEE press, Wiley, 2013.

[16] *Guide for grid interconnection of embedded generators, Part I: Application, evaluation and interconnection procedure,* Ceylon Electricity Board, December, 2000.

[17] Wikipedia, "https://en.wikipedia.org/wiki/Photovoltaic_system," 2nd October 2015. [Online].

[18] *Guide for grid interconnection of embedded generators, Part 2: Protection and operation of grid interconnection,* Ceylon Electricity Board, December, 2000.

[19] CEB, "Long term transmision development plan 2011 - 2020," Ceylon Electricity Board, July, 2011.

[20] J. Liang, G. Venayagamoorthy and R. Harley, "Wide-Area Measurement Based Dynamic Stochastic Optimal Power Flow Control for Smart Grids With High Variability and Uncertainty," *IEEEE transactions on smart grid,* vol. 3, no. No. 1, pp. 59-69, March, 2012.

[21] CEB, "http://www.ceb.lk/downloads/st_rep/stat2010.pdf," Ceylon Electricity Board. [Online]. [Accessed 12th October 2015].

[22] CEB, "http://www.ceb.lk/downloads/st_rep/stat2013.pdf," Ceylon Electricity Board. [Online]. [Accessed 12th October 2015].

[23] T. Bambaravanage, A. Rodrigo, S. Kumarawadu and N. W. A. Lidula, "Under-Frequency Load Shedding for Power Systems with High Variability and Uncertainty," in *ISPCC 2013 Proceedings of the IEEE international confrrence on Signal Processing, Computing and Control*, Solan, India, 2013.

[24] ABB, *Load Shedding Controller, PML630 Product Guide,* Vaasa, Finland: ABB, 2011.

[25] P. Mahat, Z. Chen and B. Bak-Jensen, "Underfrequency Load Shedding for an Islanded Distribution System With Distributed Generators," *IEEE transactions on Power Delivery,* vol. 25, no. No. 2, pp. 911-918, April, 2010.

[26] V. V. Terzija, "Adaptive under-frequency load sheddig based on the magnitude of the disturbance estimation," *IEEE transactions on Power Systems,* vol. 21, no. No. 3, pp. 1260-1266, 2006.

[27] M. Begovic, D. Novose, D. Karlsson, C. Henville and G. Michel, "Wide-area protection and emergncy control," *Proceedings of the IEEE,* vol. 93, no. No. 5, pp. 876-891, May, 2005.

[28] B. Delfino, S. Massucco, A. Morini, P. Scalera and F. Silvestro, "Implementation and comparison of different under frequency load-shedding schemes," *IEEE Power Engineering Society summer meeting,* pp. 307-312, 2001.

[29] P. Anderson and M. Mirheydar, "An Adaptive Method for setting under-frequency load shedding relays," *IEEE transactions o Power Systems,* vol. 7, no. No. 2, pp. 647-655, May 1992.

[30] M. Gunawardena, C. Hapuarachchi, D. Haputhanthri and I. Harshana, "Capacity Limit of the Single Largest Generator uni, to maintain power system stability through a load shedding program," Department of Electrical Engineering, University of Moratuwa, December 2011.

[31] J. R. Jones and W. D. Kirkland, "Computer Algorithm for selection of frequency relays for Load Shedding," *IEEE Computer Applications in Power,* vol. 1, no. No. 1, pp. 21-25, 1988.

[32] H. Bentarzi, A. Quadi, N. Ghout, F. Maamri and N. E. Mastorakis, "A new approach applied to adaptive centralized load shedding scheme," in *CSECS'09 Proceedings of the 8th WSEAS International Conference on Circuits, systems, electronics, control & signal processing*, Wisconsin, USA, 2009.

[33] K. Wong and B. Lau, "Algorithm for load-shedding operations in reduced generation periods," *IEE proceedings,* vol. 139, no. No. 6, pp. 478-490, November, 1992.

[34] R. Maliszewski, R. Dunlop and G. Wilson, "Frequency actuated load shedding and restoration, Part I - Philosophy," *IEEE Transactions on Power App. Syst,* Vols. PAS-90, no. No. 4, p. 1452–1459, July 1971.

[35] Network protection & automation guide: Protective relays, measurements & control, Alstom Grid, May, 2011.

[36] B. P. S. C. C. U. M. G. Simoes, "Electrical model development and validation for distributed resources," National renewable energy laboratory, Colorado, U.S.A, April, 2007.

[37] C. Muller, User's guide on the use of PSCAD, Manitoba: Manitoba HVDC research centre, 2010.

[38] P. Wilson, User's guide: A comprehensive resource for EMTDC, Manitoba: Manitoba HVDC reseaech centre Inc., 2005.

[39] Introduction to PSCAD/EMTDC, Manitoba: Manitoba HVDC Research Centre Inc., 2003.

[40] Y. S. M. I. Xi-Fan Wang, Modern power system analysis, New York, U.S.A.: Springer Science+Business Media, LLC., 2008.

[41] ECB, "Long term transmission development studies 2005-2014," Ceylon Electricity Board.

[42] Nexans, 60-500 kV High Voltage under ground power cables: XLPE insulated cables, Paris, France: Nexans.

[43] G. F. Moor, Electric cables handbook-Third Edition: BICC Cables, Oxford, UK: Blackwell Science, 1997.

[44] E. B. Joffe and K.-S. Lock, Grounds for drounding: A circuit-to-system handbook, New Jersey, USA: IEEE press; John Wiley & Sons Inc., 2010.

[45] T. Wildi, "Chapter 10; Practical transformers," in *Electrical machines, drives and power systems: Fifth edition*, New Jersey, Prentice Hall, 2002, pp. 197-224.

[46] A. v. Meier, "Gennerators," in *Electric power systems: A conceptual introduction* , New Jersey, USA, IEEE press, Wiley-Interscience, 2006, pp. Chapter 4, 85-126.

[47] S. W. Smith, in *The scientist and Engineer's Guide to Digital Signal Processing; Second Edition*, California, USA, California Technical Publishing, 1999, pp. 35-66.

[48] K. Ogata, Modern Control Engineering, Fourth Edition, New Jersey: Prentice-Hall, 2002.

[49] CEB, "Long term transmision development plan 2011 - 2020," Ceylon Electricity Board, July, 2011.

[50] PUCSL, "Generation performance in Sri Lanaka 2014," Public utilities commision of Sri Lanka, 2014.

[51] T. Bambaravanage, A. Rodrigo, S. Kumarawadu and N. W. A. Lidula, "Under-Frequency Load Shedding for Power Systems with High Variability and Uncertainty," in *ISPCC 2013 Proceedings of the IEEE international confrrence on Signal Processing, Computing and Control*, Solan, India, 2013.

[52] CEB, "Generator Interconnection of Sri Lanka," Ceylon Electricity Board.

[53] C. Huang and S. Huang, "A time-based load shedding protection for isolated power systems," *Electric Power Systems Research,* no. 52 , pp. 161-169, 1999.

[54] M. Eremia and M. Shahidehpour, Handbook of Electrical Power System Dynamics: modeling, stability & control, IEEE press, Wiley, 2013.

[55] SIEMENS, *SIPROTEC Over Current Time Protection 7SJ80; V4.6 manual.,* SIEMENS.

[56] M. Q. Ahsan, A. H. Chowdhury, S. S. Ahmed and Imamul Hassan Bhuyan, "Technique to Develop Auto Load Shedding and," *IEEE TRANSACTIONS ON POWER SYSTEMS,* vol. 27, no. 1, pp. 198-205, FEBRUARY 2012.

[57]

[58] "http://en.wikipedia.org/wiki/Photovoltaic_system," [Online]. [Accessed 2nd October 2015].

[59] CEB, "http://www.ceb.lk/downloads/st_rep/stat2011.pdf," Ceylon Electricity Board. [Online]. [Accessed 12th October 2015].

[60] CEB, "http://www.ceb.lk/downloads/st_rep/stat2012.pdf," Ceylon Electricity Board. [Online]. [Accessed 12th October 2015].

[61] H. Bevrani, A. G. Tikdari and T. Hiyama, "Power System Load Shedding: Key Issues and New Perspectives," *World academy of science, engineering and technology,* no. 65, pp. 177-182, 2010.

[62] J. Ford, H. Bevrani and G. Ledwich, "Adaptive load shedding and regional protection," *Elsevier International Journal of Electrical Power and Energy Systems,* no. 31, pp. 611-618, 2009.

[63] S. Arnborg, G. Andersson, D. J. hill and I. A. Hiskens, "On undervoltage loadshedding in power systems," *Electrical Power Systems, Elsevier Science Ltd.,* vol. 19, no. No. 2, pp. 141-149, 1997.

[64] CEB, "Long term Generation expansion plan 2015 - 2034," Ceylon Electricity Board, July 2015.

[65] "http://www.most.gov.mm/techuni/media/EP_03041_4.pdf," [Online]. [Accessed 10 March 2013].

[66]

[67] P. Mahat, Z. Chen and B. Bak-Jensen, "Control and Operation of distributed generation in distribution systems," *ScienceDirect, Electric Power Systems research ,* vol. 81, pp. pp. 495-502, 2011.

[68] T. Bambaravanage, S. K. A. Rodrigo and N. W. A. Lidula, "A New Scheme of Under Frequency Load Shedding and Islanding Operation," *Annual Transactions of IESL,* Vols. vol. 1 - Part B,, pp. 290-296, 2013.

APPENDICES

APPENDIX – I

TRANSMISSION LINES

Power system's main power corridor: Transmission lines and transformers with a two-port network.

Referring to Figure 1 (a) approximated two port transmission network and (b) phasor diagram:

V – receiving end phase voltage
E – sending end phase voltage
P – single - phase real power
Q – single - phase reactive power

$$|BC| = XI\cos\varphi = E\sin\delta$$

Hence $I\cos\varphi = \frac{E}{X}\sin\delta$

$$|AC| = XI\sin\varphi = E\cos\delta - V$$

Hence $I\sin\varphi = \frac{E}{X}\cos\delta - \frac{V}{X}$

Real power, $P = VI\cos\varphi = \frac{EV}{X}\sin\delta$

$\therefore P(\delta) = \frac{EV}{X}\sin\delta$ ⟵ power – angle characteristics

δ is known as the load angle or power angle.

Since the real power P depends on the product of phase voltages and the sine of the angle δ between their phasors. In power networks, node voltages must be within a small percentage of their nominal values. Hence such small variations cannot influence the value of real power. Large changes of real power, from negative to positive values, correspond to changes in the sin δ. The system can operate only in that part of the characteristic which is shown by a solid line in figure 3 (c). The angle δ is strongly connected with system frequency *f*; hence the pair 'P and *f*' is also strongly interrelated.

Reactive power,

$$Q = \frac{EV}{X}\cos\delta - \frac{V^2}{X}$$

$$\cos\delta = \sqrt{1 - \sin^2\delta}$$

$$Q = \sqrt{\left(\frac{EV}{X}\right)^2 - P^2} - \frac{V^2}{X}$$

Due to stability considerations, the system can operate only in that part of the characteristic which is shown by a solid line. The smaller the reactance X, the steeper the parabola; even for small changes in V, cause large changes in reactive power. Obviously the inverse relationship also takes place: a change in reactive power causes a change in voltage.

(a)

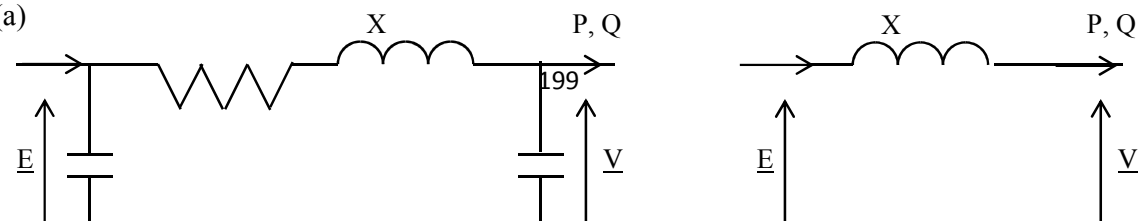

≃

(b)

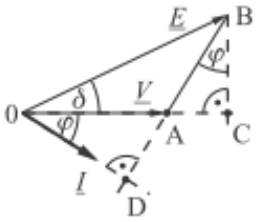

(c)

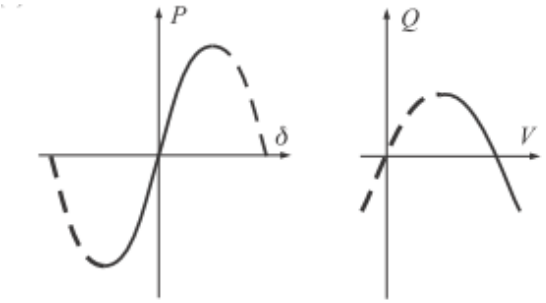

Figure1: (a) Two-port π equivalent circuit corresponding to an approximated transmission line

(b) Corresponding phasor diagram

(c) Real power and reactive power characteristics

Hence the three factors that can affect the stability of PS can be identified as:

- Load angle, δ
- Frequency, *f*
- Nodal voltage magnitude, V

APPENDIX – II

COMPOSITE LOADS

Usually each composite load represents a relatively large fragment of the system typically comprising

- low- and medium-voltage distribution networks,
- small power sources operating at distribution levels,
- reactive power compensators,
- distribution voltage regulators,
- a large number of different component loads such as motors, lighting and electrical appliances [6].

In the steady state the demand of the composite load depends on the bus-bar voltage V and the system frequency f. The functions describing the dependence of the active and reactive load demand on the voltage and frequency $P(V, f)$ and $Q(V, f)$ are called the *static load characteristics*.

The characteristics *P(V)* and *Q(V),* taken at constant frequency, are called the *voltage characteristics* while the characteristics *P(f)* and *Q(f),* taken at constant voltage, are called the *frequency characteristics.* The slope of the voltage or frequency characteristic is referred to as the *voltage (or frequency) sensitivity* of the load. Figure 2, illustrates this concept with respect to voltage sensitivities.

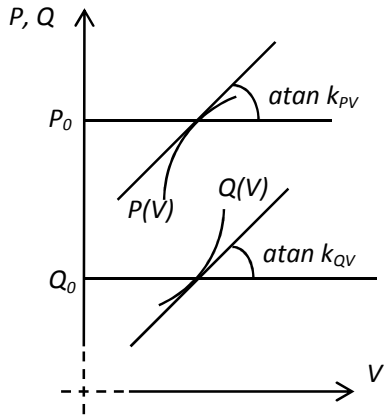

Figure 2: Illustration of the definition of voltage sensitivity

Voltage sensitivities k_{PV} and k_{QV} and the frequency sensitivities k_{PF} and k_{QF} are usually expressed in per units with respect to a given operating point:

$$k_{PV} = \frac{\Delta P/P_0}{\Delta V/V_0}$$

$$k_{QV} = \frac{\Delta Q/Q_0}{\Delta V/V_0}$$

$$k_{Pf} = \frac{\Delta P/P_0}{\Delta f/f_0}$$

$$k_{Qf} = \frac{\Delta Q/QP_0}{\Delta f/f_0}$$

Where,
P_0, Q_0, V_0, f_0, ΔP and ΔQ, are: real power, reactive power, voltage, frequency, real power change, and reactive power change at a given operating point.

A load is considered to be stiff, if at a given operating point, its voltage sensitivities are small. If,

- $k_{PV} \backsimeq 0$
  $k_{QV} \backsimeq 0$, the load is considered to be ideally stiff. The power demand of that load does not depend on the voltage.

- A load is voltage sensitive if k_{PV} and k_{QV} are high
- For a small ΔV change cause high change in the demand, ΔP .
- Usually $k_{PV} < k_{QV}$

APPENDIX – III

GENERATION CHARACTERISTIC

In the steady state, the idealized power–speed characteristic of an i[th] generating unit can be written as:

$$\frac{\Delta\omega}{\omega_n} = -\rho\frac{\Delta P_m}{P_n} \Rightarrow \frac{\Delta P_m}{P_n} = -K\frac{\Delta\omega}{\omega_n}$$

$$\frac{\Delta f}{f_n} = -\rho_i\frac{\Delta P_{mi}}{P_{ni}} \Rightarrow \frac{\Delta P_{mi}}{P_{ni}} = -K_i\frac{\Delta f}{f_n}$$

In the steady state, all the generating units operate synchronously at the same frequency. When,

$\Delta\omega$ = fraction of rated speed
ω_n = rated speed
ω = *turbine speed*
Δf = fraction of frequency
f = system frequency
ΔP_T = the overall change in the total power generated
N_G = no. of generator units
P_m = turbine power
P_n = nominal power output;

$$\Delta P_T = \sum_{i=1}^{N_G} \Delta P_{mi}$$

$$-K_i \frac{\Delta f}{f_n} = \frac{\Delta P_{mi}}{P_{ni}}$$

$$\therefore \Delta P_T = -\frac{\Delta f}{f_n} \sum_{i=1}^{N_G} K_i P_{ni}$$

$$\therefore \Delta P_T = -\Delta f \sum_{i=1}^{N_G} \left(\frac{K_i P_{ni}}{f_n}\right) \qquad (1)$$

Change in generated power as applied by the turbine

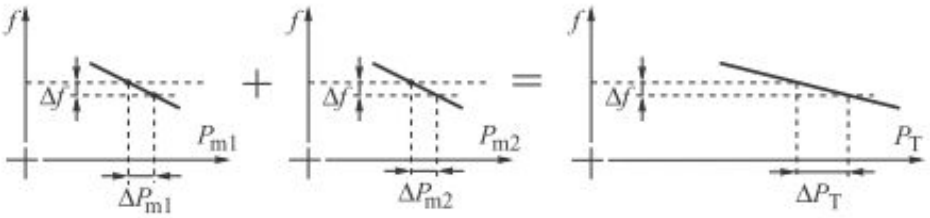

Figure 3: Generation characteristic as the sum of the speed–droop characteristics of all the generation units.

Figure 3, illustrates how the characteristics of individual generating units can be added according to Equation (1) to obtain the equivalent generation characteristic. This characteristic defines the ability of the system to compensate for a power imbalance at the cost of a deviation in frequency. For a power system with a large number of generating units, the generation characteristic is almost horizontal such that even a relatively large power change only results in a very small frequency deviation. This is one of the benefits accruing from combining generating units into one large system.

To obtain the equivalent generation characteristic of Figure 4, it has been assumed that the speed–droop characteristics of the individual turbine generator units are linear over the full range of power and frequency variations. In practice the output power of each turbine is limited by its technical parameters. The speed – droop characteristics of a turbine with an upper limit is shown in figure 4.

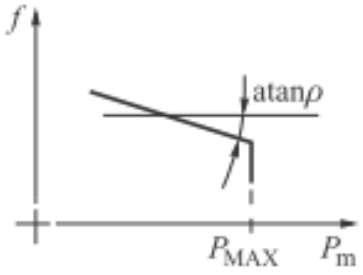

Figure 4: Speed–droop characteristic of a turbine with an upper limit.

If a turbine is operating at its upper power limit then a decrease in the system frequency will not produce a corresponding increase in its power output. At the limit $\rho = \infty$ or $K = 0$ and the turbine does not contribute to the equivalent system characteristic. Consequently the generation characteristic of the system will be dependent on the number of units operating away from their limit at part load; that is, it will depend on the spinning reserve, where **the spinning reserve is the difference between the sum of the power ratings of all the operating units and their actual load**.

The allocation of spinning reserve is an important factor in power system operation as it determines the shape of the generation characteristic. This is demonstrated in figure 6, with two generating units.

In Figure 6 (a), the spinning reserve is allocated proportionally to both units (which operate at a frequency of f_0) and the maximum power of both generators is reached at the same operating frequency f_1. The sum of both characteristics is then a straight line (as given in equation (1)), up to the maximum power $P_{MAX} = P_{MAX\,1} + P_{MAX\,2}$.

Figure 5 (b) shows a situation where the total system reserve is the same (equal to the amount of the previous case), but it is allocated solely to the second generator. That generator is loaded up to its maximum at the operating point (frequency f_2). The resulting total generation characteristic is nonlinear and consists of two lines of different slopes. The first line is formed by adding both inverse droops, $K_{T1} \neq 0$ and $K_{T2} \neq 0$, in Equation (3). The second line is formed noting that the first generator operates at maximum load and $K_{T1} = 0$, so that only $K_{T2} \neq 0$ appears in the sum in Equation (3). Hence the slope of that characteristic is higher.

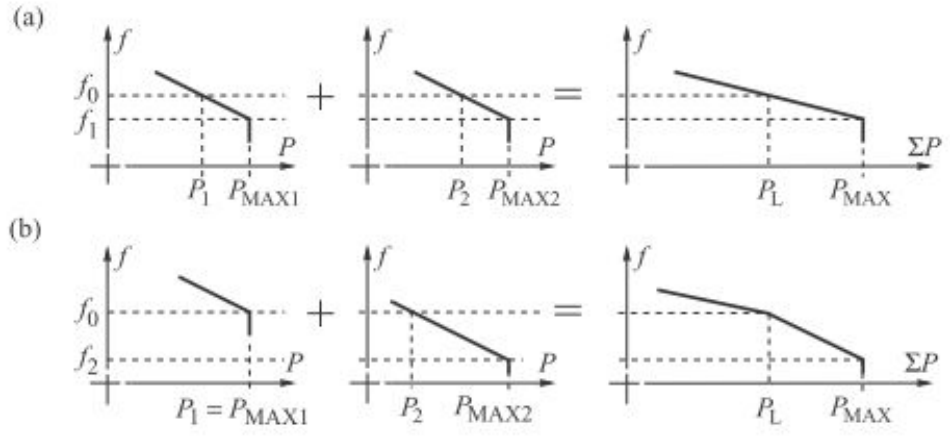

Figure 5: Influence of the turbine upper power limit and the spinning reserve allocation on the generation characteristic.

The number of units operating in a real system is large. Some of them are loaded to the maximum but others are partly loaded, generally in a non-uniform way, to maintain a spinning reserve. Adding up all the individual characteristics would give a nonlinear resulting characteristic consisting of short segments with increasingly steeper slopes. That characteristic can be approximated by a curve shown in Figure 6. The higher the system load, the higher the droop until it becomes infinite $\rho_T = \infty$, and its inverse $K_T = 0$, when the maximum power P_{MAX} is reached. If the dependence of a power station's auxiliary requirements on frequency were neglected, that part of the characteristic would be vertical (shown as a dashed line in Figure 6). However, power stations tend to have a curled-back characteristic – see curve 4 in Figure 8. Similarly curled is the system characteristic shown in Figure 6.

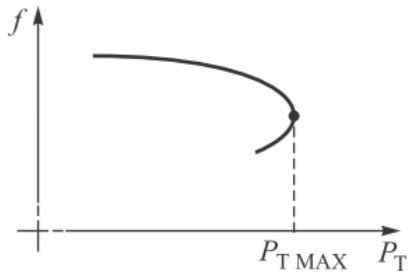

Figure 6: Static system generation characteristic

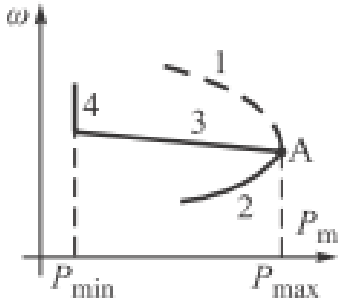

Figure 7: Turbine power–speed characteristic for the unregulated turbine (lines 1, 2) and the regulated turbine (lines 3, 2, and 4).

The generation characteristic of an actual power system is nonlinear and consists of many short sections of increasing slope as more and more generating units reach their operating limits as the total load increases until, at maximum system load, there is no more spinning reserve available. The generation characteristic then becomes a vertical line. For small power and frequency disturbances, it is convenient to approximate this nonlinear generation

characteristic in the vicinity of the operation point by a linear characteristic with a local droop value.

The total system power generation is equal to the total system load (P_L), including transmission losses.

$$\sum_{i=1}^{N_G} P_{mi} = P_L$$

Equation (1)/P_L gives:

$$\frac{\Delta P_T}{P_L} = -K_T \frac{\Delta f}{f_n} \; or \; \frac{\Delta f}{f_n} = -\rho_T \frac{\Delta P_T}{P_L} \qquad (2)$$

Where,

$$K_T = \frac{\sum_{i=1}^{N_G} (K_i P_{ni})}{P_L} \qquad (3)$$

$$\rho_T = \frac{1}{K_T}$$

Equation (2) describes the linear approximation of the generation characteristic calculated for a given total system demand. Further, the coefficients in Equation (3) are calculated with respect to the total demand, not the sum of the power ratings, so that ρ_T is the local speed-droop, of the generation characteristic and depends on the spinning reserve and its allocation in the system as demonstrated in Figure (5).

APPENDIX – IV

VOLTAGE COLLAPSE

When the reactive power required by the transmission system becomes inadequate, we say that the power system goes through a "voltage collapse." Voltage collapse can be best explained by the trivial example shown in Figure 8, [13]. If we solve the power flow equations for the load bus, we get:

$$P(V,\theta) = -V.Sin\theta.\frac{E}{X}$$

And

$$Q(V,\theta) = -V.\frac{(-Cos\theta.E + V)}{X}$$

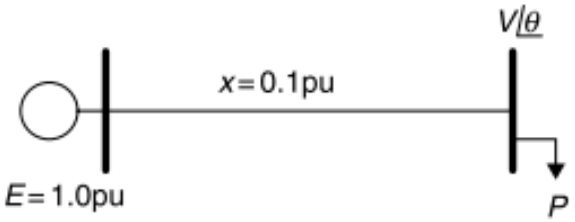

Figure 8: example power system to show voltage collapse.

If we give the relationship between Q and P as Q = tan(ϕ) · P, then we get the plot for various values of tan(ϕ) as shown in Figure 9. With reference to Figure 9, when the load draws reactive power (tan(ϕ) ≥ 0), the voltage drops off faster as P increases. Similarly, if the load produces reactive power (tan (ϕ) ≤ 0), the voltage actually rises and stays above 1.0 pu for much of the range. This is the phenomena of reactive compensation wherein one can supply more real power, P, if reactive power is supplied at the load.

During a serious emergency on the transmission system or when a generator is lost, the reactive power being consumed by the transmission system will cause the voltage to drop. More importantly, the curve, often called the "nose curve" because of its shape, contracts and the result is as shown in Figure 10.

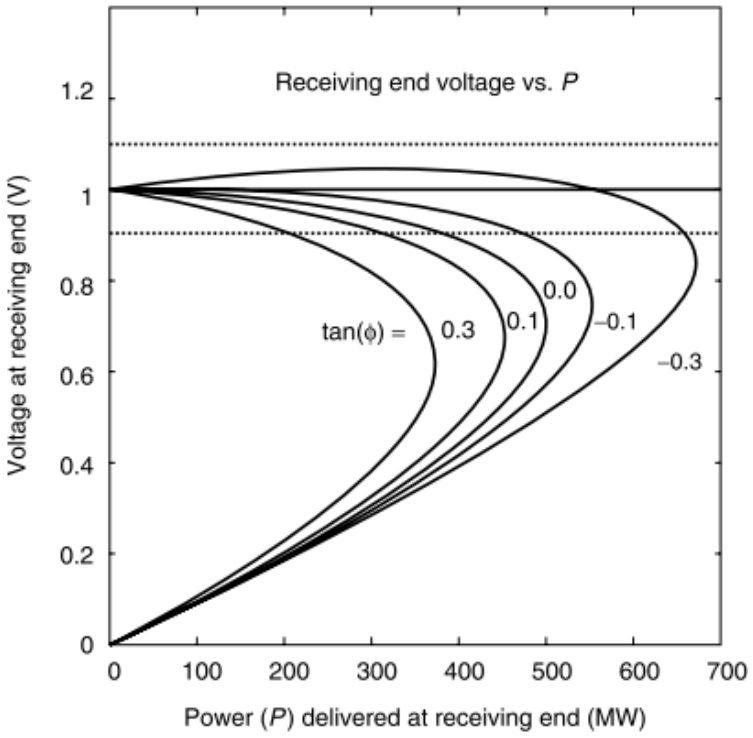

Figure 9: Voltage at receiving bus versus power delivered.

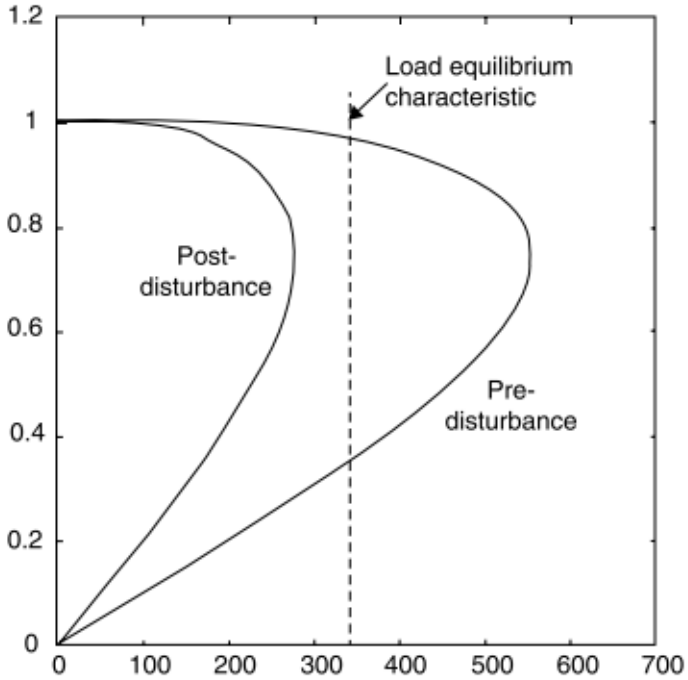

Figure 10: contraction of the voltage characteristic during a transmission outage.

In this case, we shall assume that the system was supplying about 330 MW and gave adequate reactive support to result in a pre-disturbance voltage that was within limits. The

disturbance results in loss of transmission, and the resulting new voltage characteristic no longer even intersects the vertical line at 330 MW and we then have a situation where the power flow cannot be solved. Under such conditions, the voltage will collapse and the whole power system will go down. Generally, failure of the power flow is a sign that the power system is not secure and should be alarmed to operators.

APPENDIX – V

Generation and transmission network of Sri Lanka as at 2011.

APPENDIX – VI

Swing equation [6]

Swing equation is the fundamental equation governing the rotor dynamics.

One of the natural frequencies of the turbine/generator drive system will be at 0 Hz and represents free-body rotation where the turbine and generator inertias move together with no relative displacement of the individual rotor masses. When connected to the power system this free-body rotation will appear as a low-frequency oscillation of typically 1 to 2 Hz. It is this free-body rotation that is addressed in this section. When considering free-body rotation the shaft can be assumed to be rigid when the total inertia of the rotor J is simply the sum of the individual inertias. Any unbalanced torque acting on the rotor will result in the acceleration or deceleration of the rotor as a complete unit according to Newton's second law:

$$J\frac{d\omega_m}{dt} + D_d\omega_m = \tau_t - \tau_e \qquad \text{(A)}$$

Where,
J – total moment of inertia of the turbine and generator rotor (kgm^2)
ω_m – rotor shaft velocity (mechanical rad/s)
τ_t – torque produced by the turbine (Nm)
τ_e – counteracting electromagnetic torque
D_d – damping-torque coefficient (Nms) – considers for the mechanical rotational loss due to windage & friction

In the steady state,

$$\frac{d\omega_m}{dt} = 0$$

Then, rotor angular speed = synchronous speed = ω_{sm}

$$\tau_t = D_d\omega_{sm} + \tau_e$$

∴ The net mechanical shaft torque = τ_m,

$$\tau_m = \tau_t - D_d\omega_{sm} = \tau_e$$

If, $\tau_m > \tau_e$, $then\ rotor\ accelarates.$
$\tau_m < \tau_e$, $then\ rotor\ decelarates.$

$$\omega_m = \omega_{sm} + \Delta\omega_m$$
$$\omega_m = \omega_{sm} + \frac{d\delta_m}{dt}$$

$$\frac{d\omega_m}{dt} = \frac{d}{dt}\left[\omega_{sm} + \frac{d\delta_m}{dt}\right] = \frac{d^2\delta_m}{dt^2}$$

$\therefore$ (A) $\Rightarrow$

$$J\,\frac{d^2\delta_m}{dt^2} + D_d\left[\omega_{sm} + \frac{d\delta_m}{dt}\right] = \tau_t - \tau_e$$

$$J\,\frac{d^2\delta_m}{dt^2} + D_d\frac{d\delta_m}{dt} = \underbrace{(\tau_t - D_d\omega_{sm})}_{\tau_m} - \tau_e$$

$$J\,\frac{d^2\delta_m}{dt^2} + D_d\frac{d\delta_m}{dt} = \tau_m - \tau_e$$

$$J\,\omega_{sm}\frac{d^2\delta_m}{dt^2} + D_d\omega_{sm}\frac{d\delta_m}{dt} = \omega_{sm}\tau_m - \omega_{sm}\tau_e$$

$$= \frac{\omega_{sm}}{\omega_m}\omega_m\tau_m - \frac{\omega_{sm}}{\omega_m}\omega_m\tau_e$$

$$= \frac{\omega_{sm}}{\omega_m}P_m - \frac{\omega_{sm}}{\omega_m}P_e$$

$\omega_{sm} \backsimeq \omega_m$;

Hence,

$$\underbrace{J_{sm}\,\omega_{sm}}_{M_m}\frac{d^2\delta_m}{dt^2} = P_m - P_e - \underbrace{D_d\omega_{sm}}_{D_m}\frac{d\delta_m}{dt}$$

$$M_m\,\frac{d^2\delta_m}{dt^2} = P_m - P_e - D_m\frac{d\delta_m}{dt}$$

$$\boxed{M_m\,\frac{d^2\delta_m}{dt^2} = P_m - P_e - D_m\frac{d\delta_m}{dt}} \quad \text{——— (B)}$$

Where,
$M_m = \ angular\ momentum\ of\ rotor\ at\ synchronous\ speed$
$D_m\ = damping\ coefficient$
$\omega_{sm} = synchronous\ speed$

It is common practice to express the angular momentum of the rotor in terms of a normalized inertia constant when all generators of a particular type will have similar 'inertia' values regardless of their rating.

Inertia constant, H is defined as: *The stored kinetic energy in MJ at synchronous speed divided by the machine rating, S_n in MVA*, so that:

$$H = \frac{\frac{1}{2}J\omega_{sm}^2}{S_n}$$

$$M_m = \frac{2HS_n}{\omega_{sm}}$$

$[H] = s$

H – Kinetic energy of the rotor at synchronous speed, in terms of the number of seconds it would take the generator to provide an equivalent amount of electrical energy when operating at a power output equal to its MVA rating

The power angle and angular speed can be expressed in electrical radians and electrical radians per second respectively, rather than their mechanical equivalent, by substituting

$$\delta = \frac{\delta_m}{p/2}$$

$$\omega_s = \frac{\delta\omega_{sm}}{p/2}$$

Where,
P –number of poles
δ – power angle in electrical radians
ω_s – electrical radians per second

Substituting δ and ω_s in equation (B), the swing equation can be written as,

$$\frac{2HS_n}{\omega_s}\frac{d^2\delta}{dt^2} + D\frac{d\delta}{dt} = P_m - P_e$$

$$D = \frac{2D_m}{p}$$

Let,
M – inertia coefficient
P_D – damping power
D – damping coefficient
P_{acc} – net accelerating power

Then,

$$M = \frac{2HS_n}{\omega_s}$$

$$P_D = D\frac{d\delta}{dt}$$

Then swing equation takes common form:

$$M\frac{d^2\delta}{dt^2} = P_m - P_e - P_D = P_{acc}$$

Further,

$$M\frac{d\Delta\omega}{dt} = P_m - P_e - P_D = P_{acc}$$

$$\frac{d\delta}{dt} = \Delta\omega$$

ω_m – rotor speed in mechanical rad/s
ω_e – rotor speed in electrical rad/s

The rotor angular speed is synchronous speed ω_{sm} while the turbine torque τ_t is equal to the sum of the electromagnetic torque τ_e and the damping (or rotational loss) torque $D_d\omega_{sm}$.